Study on subsynchronous resonance problem in series-compensated transmission system

Chengbing He[*], Dongchao Chen

School of energy, power and mechanical engineering, North China Electric Power University, Beijing 102206, China

Abstract

The series capacitor compensation technique can improve the transmission capability of transmission system; however, it may cause subsynchronous resonance (SSR) which will seriously influence the safe operation of large turbo-generator shafts. Aiming at a series capacitor compensation transmission system, the transient torques of SSR is simulated in different compensation degrees and unit load levels. Based on the modified segmentation Prony algorithm (MSPA) proposed in this paper, the characteristic frequencies and damping parameters are identified and analysed. The MSPA, complex Morlet wavelet and time-frequency contour map are integrated and used in analysis of transient torques of SSR in time-frequency field. The results of study show that the transient torques develop towards divergence direction and the frequencies of SSR (converted to the rotor side) in negative damping area move towards into low frequency area with the increasing of the compensation degree. With the increasing of the power output, the torque values of each shaft section will increase, but the dominant oscillation mode will not change. The increasing of power output can make the damping effect slightly change and the trend of the change develops towards the direction that is not conducive to restrain SSR.

Keywords: series-compensated transmission, subsynchronous resonance, modified segmentation Prony algorithm, complex Morlet wavelet, time-frequency contour map

1 Introduction

Series compensation is an effective and economical mean to enhance the transmission capability and improve the stability of long transmission systems, but it may cause subsynchronous resonance (SSR). The electrical-mechanical resonance phenomenon would seriously affect the safety of large turbo-generator shafts and the stability of the power system. The SSR analysis methods mainly include eigenvalue analysis, complex torque coefficient approach, time domain simulation method, Prony algorithm (PA), and so on.

PA can obtain the characteristic parameters of sampling signal easily and is applicable for SSR analysis. Most of the exiting PAs can only be applied to part of sampling signal every time, so the results are random and inaccurate [1-5]. An improved PA [6,7], which is called segmentation PA (SPA) in this paper, enhances the accuracy of the identified results by dividing the whole observation window into several segments and comparing the results of each segment obtained by PA to determine the optimal results, but it reduces the computational efficiency. More important, it is difficult to deal with and choose the results among different segments. Reference [8] reports a moving window PA (MWPA) which has stronger adaptability to noise and can be applied to long time range signals. However, it is raised on the basis of the modified PA (MPA) which uses singular value decomposition (SVD) to determine the rank of Prony model. Experimental results of this paper and reference [9]

demonstrate that the order of the model acquired by means of SVD is low, so some concerned oscillation modes sometimes cannot be obtained.

In view of the problems mentioned above, a modified SPA (MSPA) based on traditional PA (TPA) and SPA is proposed in the paper. The MSPA, complex Morlet wavelet and time-frequency contour map are integrated and used in analysis of transient torques of SSR in time-frequency field.

2 Modified segmentation Prony algorithm

PA is a method fitting a linear combination of exponential terms to a signal (N≥2p). Supposing that a signal is composed by p exponential functions, the mathematical model in discrete time function form is:

$$x_n = \sum_{k=1}^{p} A_k \exp(j\theta_k) \exp[(\sigma_k + j2\pi f_k)n\Delta t], \qquad (1)$$

where n=0,1,…,N-1; k=1,2,…,p; p is the order; Δt is the sampling time-interval; A_k, f_k, σ_k and θ_k are magnitude, frequency, attenuation factor and primary phase.

Meanwhile, the expressions of residues and pole are defined as follows:

$$b_k = A_k \exp(j\theta_k) \quad z_k = \exp[(\sigma_k + j2\pi f_k)\Delta t] \qquad (2)$$

[*] *Corresponding author* e-mail: hcbyy@126.com

Assuming that N is the number of data points in the observation window, while the number of sampling data within each segment is same as m, and the identification order of each segment is same as p (p is great enough to ensure the identification accuracy for each segment).To ensure that it is completely applicable to effective signal, there must be several repetitive data points whose number is m-p between the adjacent sections. The serial number of each segment is i and the total number of the segments is j which can be calculated by the following formula.

$$j = [(N-m)/p]_- + 1 , \qquad (3)$$

where the operator [ ]- means negative round number.

For the ith segment similar with the derivation process of TPA, the forward differential equation can be obtained and expressed as:

$$\sum_{h=0}^{p} a_h^i x_{n+h}^i = 0 , \qquad (4)$$

where x_n^i are the data points in the ith segment, i=1,2,…,j; n=0,1,…,m-p-1; a_p^i=1. Sum the two sides of equations shown as the above equation in all of the segments, and then the following formula can be obtained.

$$\sum_{i=1}^{j} \sum_{h=0}^{p} a_h^i x_{n+h}^i = 0 . \qquad (5)$$

Because a_h^i (i=1,2,…,j; h=0,1,…,p) should remain unchanged for each segment, let them be equal to a_h. Equation (5) can be transformed into Equation (6).

$$\frac{1}{j} \sum_{h=0}^{p} a_h \sum_{i=1}^{j} x_{n+h}^i = 0 . \qquad (6)$$

The Equation (7) can be constructed by Equation (6).

$$-\begin{bmatrix} X(p) \\ X(p+1) \\ \vdots \\ X(m-1) \end{bmatrix} = \begin{bmatrix} X(0) & X(1) & \cdots & X(p-1) \\ X(1) & X(2) & \cdots & X(p) \\ \vdots & \vdots & \vdots & \vdots \\ X(m-p-1) & X(m-p) & \cdots & X(m-2) \end{bmatrix} \begin{bmatrix} a_0 \\ a_1 \\ \vdots \\ a_{p-1} \end{bmatrix}, \qquad (7)$$

where $X(n)$=$(x_n^1+x_n^2+…+x_n^j)/j$; n=0,1,2,…,m-1. As shown by Equation (7), the overall sample function matrix is constructed and the average error effect of the whole observation window is taken into account in the MSPA, which are different from the exiting ones.

Using singular value decomposition and total least square method (SVD-TLS) to solve the coefficients a_h, z_k can be obtained by solving the characteristic polynomial which is presented as Equation (8).

$$Z^P + a_{p-1}Z^{P-1} + \cdots + a_1 Z + a_0 = 0 \qquad (8)$$

The MSPA residues can be computed by SVD-TLS according to the following formula.

$$\begin{bmatrix} 1 & 1 & \cdots & 1 \\ z_1 & z_2 & \cdots & z_p \\ \vdots & \vdots & \vdots & \vdots \\ z_1^{m-1} & z_2^{m-1} & \cdots & z_p^{m-1} \end{bmatrix} \begin{bmatrix} b_1^1 \\ b_2^1 \\ \vdots \\ b_p^1 \end{bmatrix} = \begin{bmatrix} x_0^1 \\ x_1^1 \\ \vdots \\ x_{m-1}^1 \end{bmatrix} . \qquad (9)$$

In term of z_k and b_k^1 (residues in the first segment), magnitude, primary phase, damping coefficient and frequency can be obtained on basis of the following formula.

$$\begin{cases} A_k = \left| b_k^1 \right| \\ \theta_k = \arctan\left[\text{Im}\left(b_k^1\right) / \text{Re}\left(b_k^1\right) \right] \\ \sigma_k = \ln\left| z_k \right| / \Delta t \\ f_k = \dfrac{\arctan\left[\text{Im}\left(z_k\right) / \text{Re}\left(z_k\right) \right]}{2\pi\Delta t} \end{cases} . \qquad (10)$$

The resonance characteristic of the power system is negative damped oscillation when σ_k is positive, and vice versa.

According to the sampling theorem, the sampling frequency 1000 Hz is adopted in the analysis of SSR. The time length of each segment is set to 2 seconds and the time length of the window 4~5 seconds is adopted and the failure period should be avoided. With regard to the rank p, the rank 100 is temporarily adopted here. Lots of interference components will emerge when p is assigned to a big value directly. The sampling signal is analysed by KW-FFT method in order to get the frequencies (F_L, L=1,2,…) of the peak points, then the oscillation modes can be preliminary screened by Equation (11).

$$\left| f_k - F_L \right| \le C , \qquad (11)$$

where C is a constant, which could be 0.5~1Hz according to practical needs.

By means of making changes to the energy class, the energy class of SSO modes is defined as:

$$E_k = A_k^2 \sum_{s=1}^{m} (e^{\sigma_k s \Delta t})^2 = \frac{A_k^2 (e^{2m\Delta t \sigma_k} - 1)}{1 - e^{-2\Delta t \sigma_k}} . \qquad (12)$$

Both magnitude and attenuation factor are taken into account in Equation (12). Near each F_L, a group of f_k can be obtained on basis of Equation (11). Their energy class can be calculated by Equation (12). And then, the mode whose energy class is the biggest among the group can be found out. It is just one of the oscillation modes.

Simulation results based on the FBM show that the MSPA presented here is suitable for the analysis of SSO and superior to the traditional ones to some extent [10].

3 Complex morlet wavelet and time-frequency contour map

The traditional FFT method is not suit for non-stationary signal analysis. The complex Morlet wavelet adopts

Gauss function, which time-frequency window area is smallest, whose localization properties of time-frequency domain are good, and the symmetry is better. The transform result can reflect both the signal amplitude and phase relationship [11, 12]. The introduction of the complex Morlet wavelet transform can provide a new means to torsional vibration monitoring and analysis.

The time-domain expression of complex Morlet wavelet can be written as:

$$\psi(t) = \frac{1}{\sqrt{\pi f_b}} \exp(j2\pi f_c t) \exp(-t^2 / f_b) , \qquad (13)$$

where, f_b is bandwidth parameter. f_c is centre frequency. The values of f_b and f_c can be adjusted according to the time-frequency resolution need in practice. The analysis result of the complex Morlet wavelet can be represented by time-frequency contour map. After the specific form of Morlet wavelet is determined, observation of a scales wavelet transform is equivalent to that of time-frequency contour map. Frequency-domain information and time-domain information are contained in time-frequency contour map that can visually not only represent the original signal energy distribution but also show the relationship between each scale wavelet coefficient [13].

4 Simulations and results

The study system is according to the conversion design of the second benchmark model for computer simulation of SSR, whose wiring diagram and parameters are given in reference [14]. The generator and shaft are replaced. The parameters of the turbo-generator come from a 600MW unit, whose shaft is four spring-mass models, including HIP, LPA, LPB and GEN. The system exhibits three torsional modes at frequencies 12.512 Hz, 20.755 Hz, and 25.646 Hz. The auxiliary power is 4% of generating unit rating.

4.1 ANALYSIS OF DIFFERENT SERIES COMPENSATION DEGREES

The simulation conditions are: generator output of P_e=0.9 p.u., terminal voltage of V_t=1.0 p.u.. It is assumed that the system is experienced by an instantaneous single phase short-circuit from 1.5 s to 1.6 s in the middle of the line which contains series compensation. The simulation lasts 10 s. Series compensation degrees (described by X_C) are respectively set as 30%, 50% and 70%.

The torque response curves in time-domain between LPB and GEN and their time-frequency contour maps in different compensation degrees are given in Figure 1, Figure 2 and Figure 3. Table1 shows the maximum torque response values in each section within ten seconds when compensation degrees are different. It is clearly indicated that the torque does not diverge when compensation degree is 30%. However, the torque curves become divergent when compensation degrees are 50%

and 70%. Based on the time-frequency contour maps, it should be noted that the former three modes are excited. The second order natural frequency of torsional vibration is the dominant oscillation mode when compensation degrees are 30% and 50% (the curves in the figures exhibit dark colour). As the compensation degree is 70%, the first step mode is the dominant oscillation mode. The results in Table1 show that the maximum torque response value appears between LPB and GEN when compensation degrees are 30% and 50%. As XC equals to 70%, the maximum torque response value appears between LPA and LPB (the maximum torque between LPB and GEN is 3.498 p.u., however, it is 5.222 p.u. between LPA and LPB). Therefore, the effect on the position of the maximum torque should be considered in the process of safety analysis on torsional vibration of turbo-generator shafts to avoid locating the wrong dangerous section.
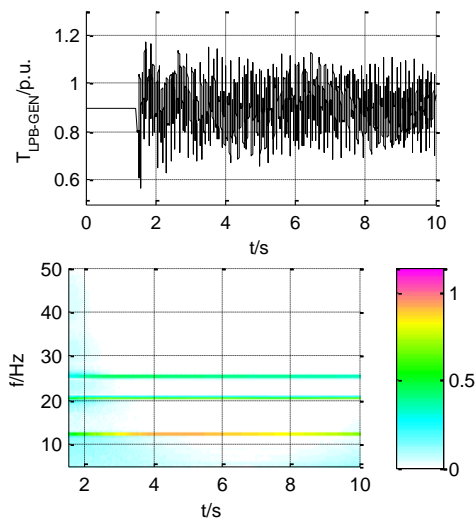
FIGURE 1 The torque response curve between LPB and GEN and its time-frequency contour map (XC=30%)
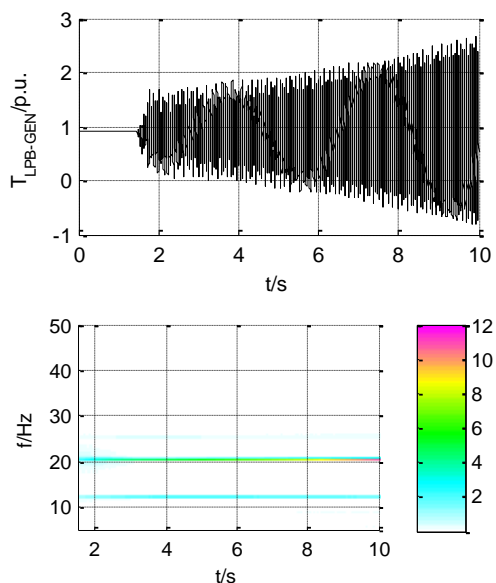
FIGURE 2 The torque response curve between LPB and GEN and its time-frequency contour map (XC=50%)
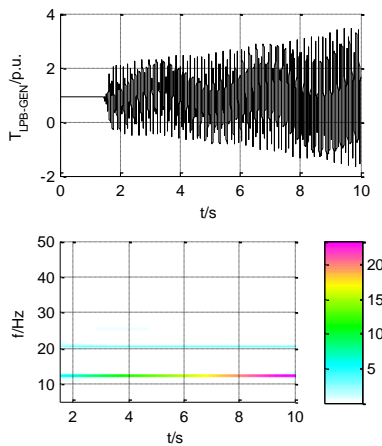
FIGURE 3 The torque response curve between LPB and GEN and its time-frequency contour map (XC=70%)

TABLE 1 The maximum torque response values within ten seconds when compensation degrees are different

	X_C=30%	X_C=50%	X_C=70%
$T_{HIP-LPA}$/p.u.	0.928	1.122	1.609
$T_{LPA-LPB}$/p.u.	1.038	1.826	**5.222**
$T_{LPB-GEN}$/p.u.	1.172	**2.691**	3.498

Table 2 shows the results of the torques between LPB and GEN under the different series compensation degrees analyzed by MSPA. As shown in the table, all of the torsional vibration frequencies can be correctly recognized. When the series compensation degree is 30%, the modes at different frequencies have the positive damping, so the torque response curve is damped. As the series compensation degree is 50%, the modal damping at the second order frequency is negative and the torque curve appears to oscillation and divergence. As the series compensation degree is 70%, the modal damping at the first order frequency is negative and the torque curve appears to oscillation and divergence. The frequencies of SSR (converted to the rotor side) in negative damping area move towards into low frequency area with the increasing of the compensation degree. Therefore, in order to prevent the happening of SSR, the series compensation degrees must be designed reasonably in the new transmission projects to avoid torsional natural frequencies.

TABLE 2 The results of the torques (TLPB-GEN) under the different compensation degrees analysed by MSPA

	f/Hz			σ		
X_C	*30%*	*50%*	*70%*	*30%*	*50%*	*70%*
Mode1	12.620	12.628	12.642	-0.0346	-0.0184	**0.1278**
Mode2	20.841	20.826	20.822	-0.0009	**0.1314**	-0.0024
Mode3	25.634	25.635	25.632	-0.0356	-0.0496	-0.0383

4.2 ANALYSIS OF VARIOUS POWER OUTPUTS

The simulation conditions are: series compensation degree of XC=50%, terminal voltage of Vt=1.0 p.u.. It is assumed that the system is experienced by an instantaneous single phase short-circuit from 1.5 s to 1.6 s in the middle of the line which contains series compensation. The simulation lasts 10 s. Power outputs

(described by Pe) are respectively set as 0.3 p.u., 0.6 p.u. and 0.9 p.u.. The torque response curve and time-frequency contour map are illustrated in Figure 2.

The torque between LPB and GEN response curves and their time-frequency contour maps for Pe=0.3 p.u. and Pe=0.6 p.u. are given in Figure 4 and Figure 5. The maximum torque response values in each section within ten seconds when power outputs are different and the results of the torque between LPB and GEN based on MSPA are shown in Table 3 and Table 4. It can be seen from the figures that all of torque response curves are divergent and the second step mode is the dominant oscillation mode. With the increasing of power output, the maximum torque response values in each section are also getting higher. All of the maximum torque response values appear between LPB and GEN, at the same time, the dominant oscillation mode of the torque has no change. In other words, the dominant oscillation mode will not change when power output is changed. However, in view of the attenuation factors, the increasing of power output can make the damping effect slightly change and the trend of the change develops towards the direction that is not conducive to restrain SSR.
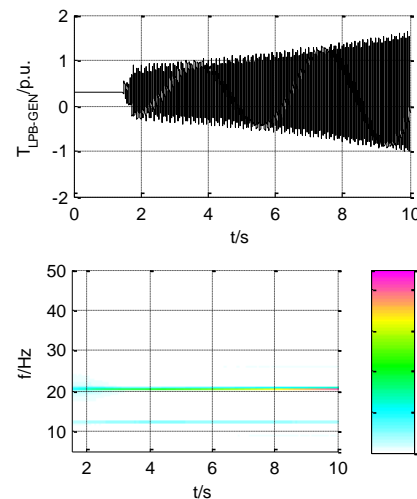
FIGURE 4 The torque response curve between LPB and GEN and its time-frequency contour map (Pe=0.3p.u.)
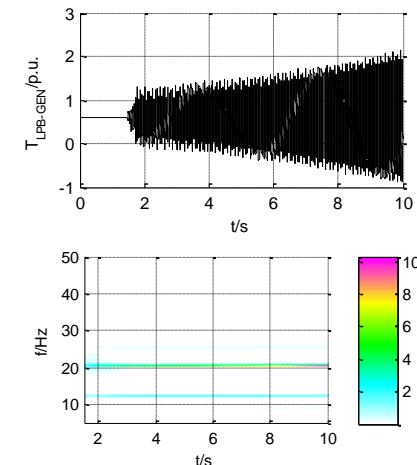
FIGURE 5 The torque response curve between LPB and GEN and its time-frequency contour map (Pe=0.6p.u.)

TABLE 3 The maximum torque response values within ten seconds when power outputs are different

	P$_e$=0.3p.u.	P$_e$=0.6p.u.	P$_e$=0.9p.u.
T$_{HIP-LPA}$/p.u.	0.523	0.820	1.122
T$_{LPA-LPB}$/p.u.	0.941	1.334	1.826
T$_{LPB-GEN}$/p.u.	1.615	2.131	2.691

TABLE 4 The results of the torques (TLPB-GEN) under the different power outputs analysed by MSPA

	f/Hz			σ		
P$_e$/p.u.	0.3	0.6	0.9	0.3	0.6	0.9
Mode1	12.63	12.635	12.628	-0.0434	-0.0319	-0.0184
Mode2	20.83	20.832	20.826	**0.1107**	**0.1199**	**0.1314**
Mode3	25.63	25.635	25.635	-0.0607	-0.0530	-0.0496

5 Conclusions

The series capacitor compensation technique can cause SSR which will seriously influence the safe operation of large turbo-generator shafts. The transient torques of SSR are simulated in different compensation degrees and unit load levels in the paper. Based on the modified segmentation Prony algorithm proposed in this paper, the characteristic frequencies and damping parameters are identified and analysed. The MSPA, complex Morlet wavelet and time-frequency contour map are integrated and used in analysis of transient torques of SSR in time-frequency field. The achievements of this dissertation are mainly as follows: (1) The second order natural frequency of torsional vibration is the dominant oscillation mode when compensation degrees are 30% and 50%. As the compensation degree is 70%, the first step mode is the dominant oscillation mode. (2) The transient torques develops towards divergence direction and the frequencies of SSR (converted to the rotor side) in negative damping area move towards into low frequency area with the increasing of the compensation degree. (3) With the increasing of power output, the maximum torque response values in each section are also getting higher. All of the maximum torque response values appear between LPB and GEN. (4) The dominant oscillation mode will not change when power output is changed. However, the increasing of power output can make the damping effect slightly change and the trend of the change develops towards the direction that is not conducive to restrain SSR.

Acknowledgments

References

[1] Jaroslaw Z, Janusz M 2011 *Metrology and measurement systems* **18**(3) 371-8

[2] Shim K S, Nam H K, Lim Y C 2011 *European transactions on electrical power* **21**(5) 1746-62

[3] Maergoiz L S 2008 *Doklady mathematics* **78**(3) 822-4

[4] Jaroslaw Z, Janusz M 2012 *Metrology and measurement systems* **19**(3) 489-98

[5] Deng J X, Tu J, Chen W H 2007 *Power System Technology* **31**(7) 36-41

[6] Dong H, Liu D C, Zou J F 2006 *High Voltage Engineering* **32**(6) 97-100

[7] Nam S R, Lee D G, Kang S H 2011 *Journal of electrical engineering & technology* **6**(2) 154-60

[8] Ding L, Xue A C, Li J 2010 *Automation of Electric Power Systems* **34**(22) 24-8

[9] Barone P, Massaro E, Polichetti A 1989 *Astronomy and Astrophysics* **209**(1) 435-44

[10] Gu Y J, Chen D C, Jin T Z 2011 *Lecture Notes in Electrical Engineering* **100**(4) 211-7

[11] Kim J H, Park B Y, Akram F 2013 *Sensors* **13**(3) 3724-38

[12] Jiang D X, Diao J H, Zhao G 2005 *Proceedings of the CSEE* **25**(6) 146-51

[13] He P Li P, Sun H Q 2011 *Procedia Engineering* **15** 464-68

[14] IEEE Subsynchronous Resonance Working Group 1985 *IEEE Transactions on Power Apparatus and Systems* **104**(5) 1565-72

Authors

Chengbing He, born in October, 1974, Sichuan, China

Current position, grades: an associate professor in the School of energy, power and mechanical engineering at North China Electric Power University (NCEPU)
University studies: the Ph.D. degree in Thermal power Engineering from NCEPU
Scientific interest: on-line monitoring and analyse of coupled bending and torsional vibrations, fault diagnose of thermal equipment in power plant, and state maintenance of thermal equipment, etc.
Publications: 31

Dongchao Chen, born in December, 1985, Jilin, China

Current position, grades: the Ph.D. candidate in the School of energy, power and mechanical engineering at North China Electric Power University (NCEPU)
University studies: the bachelor's degree in Thermal and Power Engineering and the master's degree in Thermal Engineering from NCEPU
Scientific interest: On-line monitoring of coupled bending and torsional vibrations, fault diagnose of thermal equipment in power plant.
Publications: 2